

## Use of a Designed Triple-Stranded Antiparallel $\beta$ -Sheet To Probe $\beta$ -Sheet Cooperativity in Aqueous Solution

Heather L. Schenck and Samuel H. Gellman\*

Department of Chemistry, University of Wisconsin  
Madison, Wisconsin 53706

Received November 21, 1997

Cooperativity is a defining characteristic of protein tertiary structure; partially folded forms are usually less stable than either the native conformation or the denatured state.<sup>1</sup> Cooperativity can also occur at the secondary structure level: a single long segment of  $\alpha$ -helix is more stable than several short segments of equivalent total length.<sup>2</sup> Is  $\beta$ -sheet formation cooperative? It has been impossible to address this question experimentally, although cooperativity has been predicted.<sup>3</sup> Helical cooperativity is one-dimensional, while there are two possible dimensions of  $\beta$ -sheet cooperativity, perpendicular to the strand direction (Figure 1a) and along the strand direction (Figure 1b). Here we describe a 20-residue peptide that adopts a triple-stranded antiparallel  $\beta$ -sheet conformation in aqueous solution, and the use of this model system to show that antiparallel  $\beta$ -sheet formation is cooperative perpendicular to the strand direction (Figure 1a).

Elucidation of the factors that influence  $\beta$ -sheet stability has lagged behind analogous  $\alpha$ -helix studies, because it is difficult to generate soluble  $\beta$ -sheet model peptides,<sup>4</sup> while short peptides that form monomeric  $\alpha$ -helices in solution are readily available.<sup>5</sup> Intrinsic residue  $\beta$ -sheet propensities and contributions of side chain–side chain interactions to  $\beta$ -sheet stability have recently been explored using small engineered proteins that contain a solvent-exposed  $\beta$ -sheet.<sup>6</sup> This approach may not be amenable to the study of cooperativity, however, because the tertiary context is likely to mask cooperativity at the secondary structure level.

In proteins, the minimum increment of antiparallel  $\beta$ -sheet is a “ $\beta$ -hairpin”, in which two  $\beta$ -strands are connected by a short loop. This motif provides a basis for design of context-free  $\beta$ -sheet model systems. Several short, linear peptides that display partial  $\beta$ -hairpin folding in aqueous solution have been reported.<sup>7</sup> Only recently, however, has rational control of the position and size of the  $\beta$ -hairpin loop been demonstrated. Short peptides containing a central Asn–Gly (NG) or D-Pro–Xxx ( $^{\text{D}}\text{PX}$ ) segment adopt a  $\beta$ -hairpin with a two-residue loop at NG<sup>8</sup> or  $^{\text{D}}\text{PX}$ .<sup>9</sup> Both the NG and  $^{\text{D}}\text{PX}$  strategies were inspired by the observation that  $\beta$ -hairpins with two-residue loops in crystalline proteins often have a type I' or II'  $\beta$ -turn at the loop.<sup>10</sup> The D-proline strategy<sup>9,11</sup> is

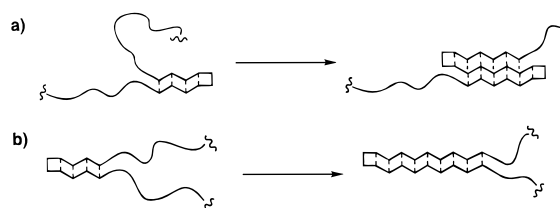


**Figure 1.** Two dimensions of propagation possible for an antiparallel  $\beta$ -sheet: (a) perpendicular to the strand direction; (b) along the strand direction.

particularly useful for the type of study reported here, because negative controls are readily available: replacing D-proline with L-proline disrupts  $\beta$ -hairpin folding.<sup>9a–c</sup>

Cooperativity perpendicular to the strand direction can be probed with a peptide that forms a triple-stranded sheet. Ac-VFITS $^{\text{D}}\text{PGKTYTEV}^{\text{D}}\text{PGOKILQ-NH}_2$  (abbreviated  $^{\text{D}}\text{P}^{\text{D}}\text{P}$ ) fulfills this requirement in aqueous solution. The two D-Pro–Gly segments are intended to adopt type II'  $\beta$ -turns, thereby promoting formation of two  $\beta$ -hairpins with one strand in common.  $^{\text{D}}\text{P}^{\text{D}}\text{P}$  was designed to bear a net charge of  $\geq +2$  (at pH 4), to discourage aggregation. Replacement of either D-Pro with L-Pro, to generate  $^{\text{L}}\text{P}^{\text{D}}\text{P}$  and  $^{\text{D}}\text{P}^{\text{L}}\text{P}$ , should abolish one  $\beta$ -hairpin; if  $\beta$ -sheet formation is cooperative perpendicular to the strand direction, then the stability of the  $\beta$ -hairpin centered on the remaining D-Pro will be attenuated in  $^{\text{L}}\text{P}^{\text{D}}\text{P}$  and  $^{\text{D}}\text{P}^{\text{L}}\text{P}$ .

Circular dichroism data show that  $^{\text{D}}\text{P}^{\text{D}}\text{P}$ ,  $^{\text{L}}\text{P}^{\text{D}}\text{P}$ ,  $^{\text{D}}\text{P}^{\text{L}}\text{P}$ , and  $^{\text{L}}\text{P}^{\text{L}}\text{P}$  behave as expected in aqueous solution at 24 °C.<sup>12</sup>  $^{\text{D}}\text{P}^{\text{D}}\text{P}$  displays a  $\beta$ -sheet signature, with a minimum at 217 nm and a zero-crossing at 205 nm.  $^{\text{L}}\text{P}^{\text{L}}\text{P}$  appears to be largely random coil, while  $^{\text{L}}\text{P}^{\text{D}}\text{P}$  and  $^{\text{D}}\text{P}^{\text{L}}\text{P}$  display signatures that are intermediate between those of  $^{\text{D}}\text{P}^{\text{D}}\text{P}$  and  $^{\text{L}}\text{P}^{\text{L}}\text{P}$ . Analytical ultracentrifugation indicated that each of the peptides is monomeric under the conditions used for spectroscopic studies. Sedimentation equilibrium data suggested molecular weights of 1500–2100 for these peptides, somewhat below the expected molecular weight of 2235 (plots of  $\ln(\text{abs})$  vs  $\text{radius}^2$  were linear at 42 K and 56 K rpm). Deviations of this type have previously been observed for designed  $\beta$ -hairpins and may reflect nonideality resulting from the net charge on these small peptides.<sup>7c</sup>

Site-specific conformational data from NMR spectroscopy (NOESY<sup>13</sup>) allowed us to assess  $\beta$ -sheet cooperativity, via comparisons among  $^{\text{D}}\text{P}^{\text{D}}\text{P}$  and its diastereomers. The numerous long-range NOEs observed for  $^{\text{D}}\text{P}^{\text{D}}\text{P}$  (Figure 2) provide strong evidence that each of the two  $\beta$ -hairpins is highly populated in aqueous solution at 24 °C. Figure 2a shows that within each  $\beta$ -hairpin of  $^{\text{D}}\text{P}^{\text{D}}\text{P}$ , characteristic cross-strand NH $\cdots$ NH NOEs are observed for the innermost pair of hydrogen-bonded amide protons (Ser-5 $\cdots$ Lys-8 and Val-13 $\cdots$ Orn-16) and for the next pair out from the  $\beta$ -turns (Ile-3 $\cdots$ Tyr-10 and Thr-11 $\cdots$ Ile-18). No NOE is observed for either of the outermost hydrogen-bonded pairs (Val-1 $\cdots$ Glu-12 or Thr-9 $\cdots$ Gln-20), which suggests that the open hairpin ends are frayed. Figure 2a shows also that three of the four possible  $\text{H}_\alpha\cdots\text{H}_\alpha$  NOEs are observed for  $^{\text{D}}\text{P}^{\text{D}}\text{P}$ , Phe-2 $\cdots$ Thr-11, Thr-4 $\cdots$ Thr-9, and Tyr-10 $\cdots$ Leu-19. The expected

(9) (a) Haque, T. S.; Little, J. C.; Gellman, S. H. *J. Am. Chem. Soc.* **1994**, *116*, 4105. (b) Haque, T. S.; Little, J. C.; Gellman, S. H. *J. Am. Chem. Soc.* **1996**, *118*, 6975. (c) Haque, T. S.; Gellman, S. H. *J. Am. Chem. Soc.* **1997**, *119*, 2303. (d) Karle, I. L.; Awasthi, S. K.; Balam, P. *Proc. Natl. Acad. Sci. U.S.A.* **1996**, *93*, 8189.

(10) Sibanda, B. L.; Thornton, J. M. *J. Mol. Biol.* **1993**, *229*, 428 and references therein.

(11) For other uses of D-proline in protein design, see: (a) Yan, Y.; Erickson, B. W. *Protein Sci.* **1994**, *3*, 1069. (b) Struthers, M. D.; Cheng, R. P.; Imperiali, B. *Science* **1996**, *271*, 342.

(12) Data in the Supporting Information.

(13) Macura, S.; Ernst, R. R. *Mol. Phys.* **1980**, *41*, 95.

(1) Creighton, T. E. *Proteins: Structures and Molecular Principles*, 2nd ed.; Freeman: New York, 1993.

(2) Qian, H.; Schellman, J. A. *J. Phys. Chem.* **1992**, *96*, 3987.

(3) (a) Mattice, W. L. The  $\beta$ -sheet to coil transition. *Annu. Rev. Biophys. Biophys. Chem.* **1989**, *18*, 93. (b) Yang, A.-S.; Honig, B. *J. Mol. Biol.* **1995**, *252*, 366.

(4) (a) Osterman, D. G.; Kaiser, E. T. *J. Cell. Biochem.* **1985**, *29*, 57. (b) DeGrado, W. F.; Lear, J. D. *J. Am. Chem. Soc.* **1985**, *107*, 7684.

(5) (a) Scholtz, J. M.; Baldwin, R. L. *Annu. Rev. Biophys. Biomol. Struct.* **1992**, *21*, 95. (b) Kemp, D. S.; Oslick, S. L.; Allen, T. J. *J. Am. Chem. Soc.* **1996**, *118*, 4249.

(6) (a) Kim, C. A.; Berg, J. M. *Nature* **1993**, *362*, 267. (b) Minor, D. L.; Kim, P. S. *Nature* **1994**, *371*, 264. (c) Smith, C. K.; Regan, L. *Science* **1995**, *270*, 980. (d) Blasie, C. A.; Berg, J. M. *Biochemistry* **1997**, *36*, 6218.

(7) (a) Blanco, F. J.; Jiménez, M. A.; Herranz, J.; Rico, M.; Santoro, J.; Nieto, J. L. *J. Am. Chem. Soc.* **1993**, *115*, 5887. (b) Tsang, K. Y.; Diaz, H.; Graciani, N.; Kelly, J. W. *J. Am. Chem. Soc.* **1994**, *116*, 3988. (c) Blanco, F. J.; Rivas, G.; Serrano, L. *Nat. Struct. Biol.* **1994**, *1*, 584. (d) Searle, M. S.; Williams, D. H.; Rackman, L. C. *Nat. Struct. Biol.* **1995**, *2*, 999.

(8) (a) Ramirez-Alvarado, M.; Blanco, F. J.; Serrano, L. *Nat. Struct. Biol.* **1996**, *3*, 604. (b) de Alba, E.; Jimenez, M. A.; Rico, M. *J. Am. Chem. Soc.* **1997**, *119*, 175. (c) Maynard, A. J.; Searle, M. S. *J. Chem. Soc., Chem. Commun.* **1997**, 1297.

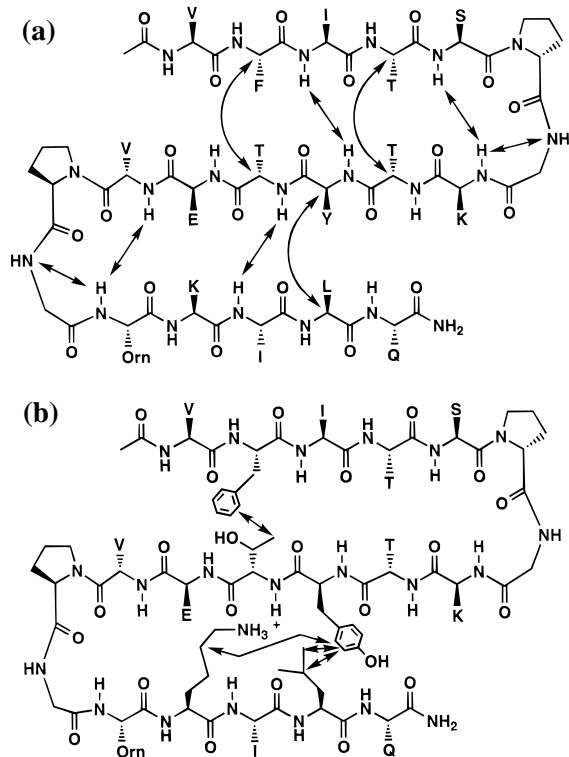


**Figure 2.** Long-range NOEs observed in NOESY analysis for 4 mM  $^{\text{D}}\text{P}^{\text{D}}\text{P}$  in 100 mM aqueous sodium deuterioacetate buffer, pH 3.8 (uncorrected), 24 °C. (a)  $\text{NH}\cdots\text{NH}$  and  $\text{H}_{\alpha}\cdots\text{H}_{\alpha}$  NOEs (the former obtained in 9:1  $\text{H}_2\text{O}:\text{D}_2\text{O}$  and the latter in  $\text{D}_2\text{O}$ ). (b) NOEs involving side chains (obtained in 9:1  $\text{H}_2\text{O}:\text{D}_2\text{O}$ ). Only unambiguously assigned NOEs are shown. Nine additional long-range NOEs were observed, all involving side chains, but resonance overlap interfered with assignment. Seven of these ambiguous NOEs could be consistent with the triple-stranded conformation. Resonance assignments were obtained from a combination of COSY and TOCSY data and sequential NOEs from ROESY data. NOESY and ROESY spectra were collected using 200 ms mixing times; NOE intensity buildup was linear between 80 and 200 ms. Orn = ornithine.

$\text{H}_{\alpha}\cdots\text{H}_{\alpha}$  NOE between Glu-12 and Lys-17, if present, would be obscured by the solvent resonance. Figure 2b shows that each  $\beta$ -hairpin displays side chain–side chain NOEs between residues well removed from the turn segment: Tyr-10 $\cdots$ Leu-19 and Tyr-10 $\cdots$ Lys-17 in the C-terminal  $\beta$ -hairpin and Phe-2 $\cdots$ Thr-11 in the N-terminal  $\beta$ -hairpin.

NOESY data for  $^{\text{L}}\text{P}^{\text{D}}\text{P}$  and  $^{\text{D}}\text{P}^{\text{L}}\text{P}$  (not shown) suggest that disrupting one  $\beta$ -hairpin diminishes the population of the remaining  $\beta$ -hairpin. As expected, the long-range NOEs diagnostic of the N-terminal  $\beta$ -hairpin are entirely absent for  $^{\text{L}}\text{P}^{\text{D}}\text{P}$ , and the long-range NOEs diagnostic of the C-terminal  $\beta$ -hairpin are absent for  $^{\text{D}}\text{P}^{\text{L}}\text{P}$ . In each case, many of the long-range NOEs within the  $\beta$ -hairpin centered on the remaining D-Pro are still observed. For both  $^{\text{L}}\text{P}^{\text{D}}\text{P}$  and  $^{\text{D}}\text{P}^{\text{L}}\text{P}$ , however, the outermost  $\text{NH}\cdots\text{NH}$  NOE of the remaining  $\beta$ -hairpin is absent (Thr-11 $\cdots$ Ile-18 and Ile-3 $\cdots$ Tyr-10, respectively). Furthermore, for  $^{\text{D}}\text{P}^{\text{L}}\text{P}$ , neither of the  $\text{H}_{\alpha}\cdots\text{H}_{\alpha}$  NOEs expected in the N-terminal  $\beta$ -hairpin, Phe-2 $\cdots$ Thr-11 or Thr-4 $\cdots$ Thr-9, is observed (the latter is near the residual water resonance, and could be obscured by solvent suppression). These remote effects of replacing one D-Pro of  $^{\text{D}}\text{P}^{\text{D}}\text{P}$  with L-Pro suggest that the two  $\beta$ -hairpins of  $^{\text{D}}\text{P}^{\text{D}}\text{P}$  reinforce one another, i.e., that the triple-stranded  $\beta$ -sheet is cooperatively stabilized.

Chemical shift data for  $\alpha$ -protons ( $\delta_{\alpha\text{H}}$ ) provide further evidence that  $^{\text{D}}\text{P}^{\text{D}}\text{P}$  adopts a triple-stranded antiparallel  $\beta$ -sheet conformation in aqueous solution and that  $\beta$ -sheet formation is cooperative perpendicular to the strand direction. Secondary structure has a profound effect on  $\delta_{\alpha\text{H}}$ ,<sup>14</sup> with  $\beta$ -sheet protons downfield-shifted

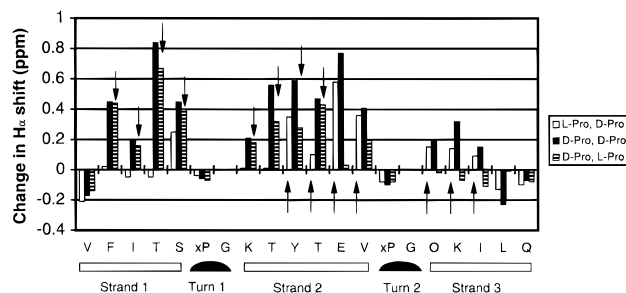


**Figure 3.**  $\Delta\delta_{\alpha\text{H}} = \text{observed } \delta_{\alpha\text{H}} - \text{random coil } \delta_{\alpha\text{H}}$  for ca. 4 mM  $^{\text{D}}\text{P}^{\text{D}}\text{P}$  (filled),  $^{\text{L}}\text{P}^{\text{D}}\text{P}$  (open), and  $^{\text{D}}\text{P}^{\text{L}}\text{P}$  (hashed) in aqueous (9:1  $\text{H}_2\text{O}:\text{D}_2\text{O}$ ) sodium deuterioacetate buffer, pH 3.8 (uncorrected), 24 °C. (See ref 14b for random coil values. The reported random coil value for lysine was used for ornithine. This extrapolation is supported by the observation that  $\delta_{\alpha\text{H}}$  for Orn-16 in  $^{\text{D}}\text{P}^{\text{L}}\text{P}$  is very near the lysine random coil value.) No data are shown Gly-7 or Gly-15 because there are two  $\text{H}_{\alpha}$  resonances in most cases; the glycine  $\Delta\delta_{\alpha\text{H}}$  values lie between  $-0.4$  and  $+0.2$  for all three peptides. Chemical shifts were externally referenced to sodium 2,2-dimethyl-2-silapentane-5-sulfonate (DSS).

and  $\alpha$ -helix protons upfield-shifted relative to the random coil. Figure 3 shows  $\Delta\delta_{\alpha\text{H}} = (\text{observed } \delta_{\alpha\text{H}} - \text{random coil } \delta_{\alpha\text{H}})$  values for  $^{\text{D}}\text{P}^{\text{D}}\text{P}$ ,  $^{\text{L}}\text{P}^{\text{D}}\text{P}$ , and  $^{\text{D}}\text{P}^{\text{L}}\text{P}$  at 24 °C. The data for  $^{\text{D}}\text{P}^{\text{D}}\text{P}$  are consistent with the proposed triple-stranded  $\beta$ -sheet conformation, since the segments Phe-2 to Ser-5 (N-terminal strand), Lys-8 to Val-13 (central strand), and Orn-16 to Ile-18 (C-terminal strand) all display  $\Delta\delta_{\alpha\text{H}} > +0.1$ . For  $^{\text{L}}\text{P}^{\text{D}}\text{P}$ , all but one residue (Ser-5) in the N-terminal strand region display random coil  $\Delta\delta_{\alpha\text{H}}$  values, which indicates that the N-terminal  $\beta$ -hairpin has been disrupted. The C-terminal  $\beta$ -hairpin still appears to form, but to a lesser extent than in  $^{\text{D}}\text{P}^{\text{D}}\text{P}$ , because the  $\Delta\delta_{\alpha\text{H}}$  values for segments Lys-8 to Val-13 and Orn-16 to Ile-18 of  $^{\text{L}}\text{P}^{\text{D}}\text{P}$  are consistently smaller than those for the corresponding residues of  $^{\text{D}}\text{P}^{\text{D}}\text{P}$  (upper set of arrows in Figure 3). Analogous behavior is observed for  $^{\text{D}}\text{P}^{\text{L}}\text{P}$ : residues in the C-terminal strand of this diastereomer display random coil  $\Delta\delta_{\alpha\text{H}}$  values, and the  $\Delta\delta_{\alpha\text{H}}$  values for the residues in the N-terminal  $\beta$ -hairpin are diminished relative to those of  $^{\text{D}}\text{P}^{\text{D}}\text{P}$  (Phe-2 to Ser-5 and Lys-8 to Val-13; lower set of arrows in Figure 3). Thus, the  $\Delta\delta_{\alpha\text{H}}$  data support the conclusion that abolishing one hairpin diminishes the population of the other.

The remote structural effects of replacing replacing D-Pro with L-Pro at either turn site in our 20-residue sequence demonstrate that the triple-stranded sheet conformation is at least partially populated for  $^{\text{D}}\text{P}^{\text{D}}\text{P}$ , and these remote effects indicate that antiparallel  $\beta$ -sheet formation is cooperative perpendicular to the strand direction. This cooperativity probably arises at least in part from entropic effects: since the C-terminal  $\beta$ -hairpin of  $^{\text{D}}\text{P}^{\text{D}}\text{P}$  is highly populated, the central strand is preorganized to engage in  $\beta$ -sheet formation with the N-terminal strand, and vice versa. Quantitative analysis of  $\beta$ -sheet cooperativity in aqueous solution is underway in our laboratory.<sup>15,16</sup>

**Supporting Information Available:** Circular dichroism data (1 page). See any current masthead page for ordering information and Web access instructions.

JA973984+

(14) (a) Wishart, D. S.; Sykes, B. D.; Richards, F. M. *Biochemistry* **1992**, *31*, 1647. (b) Wüthrich, K. *NMR of Proteins and Nucleic Acids*; Wiley: New York, 1986.

(15) After our studies were completed, a related paper appeared: Sharman, G. J.; Searle, M. S. *J. Chem. Soc., Chem. Commun.* **1997**, 1955. These workers describe a 24-residue sequence, containing two NG turn segments, that adopts a triple-stranded antiparallel  $\beta$ -sheet in 50% aqueous methanol. This peptide does not appear to display  $\beta$ -sheet folding in the absence of an organic solvent.

(16) This research was supported by the Army Research Office. H.L.S. is grateful for a National Research Service Award (T32 GM08923) from NIH. Peptides were characterized with a MALDI-TOF mass spectrometer (NSF CHE-9520868). NMR spectrometers were purchased in part through grants NSF CHE-8813550 and NIH 1 S10 RR04981. We thank Dr. Darrell McCaslin, of the UW Biophysics Instrumentation Facility, for assistance with the CD and analytical ultracentrifugation measurements (NSF BIR-9512577).